MCM-41 Supported Cu−Mn Catalysts for Catalytic Oxidation of Toluene at Low Temperatures

W. B. Li,*,†,‡ M. Zhuang,† T. C. Xiao,‡ and M. L. H. Green‡

Department of Environmental Science and Engineering, Tsinghua University, Beijing 100084, P. R. China, and Inorganic Chemistry Laboratory, University of Oxford, Oxford, OX1 3QR, United Kingdom

Received: June 8, 2006; In Final Form: August 18, 2006

Complete catalytic oxidation of toluene was investigated on Cu−Mn doped mesoporous and microporous catalysts, i.e., Cu−Mn/MCM-41, Cu−Mn/β-zeolite, Cu−Mn/ZSM-5 (where SiO_2/Al_2O_3 is either 25 or 38), and Cu−Mn/porous silica, in the presence of excess oxygen. The result shows that mesoporous catalysts have exhibited the highest catalytic activity among these catalysts above. The less amount of coke formation due to the unique mesoporous structures could play a key role in the high activity on the mesoporous catalyst. In addition, the bimetallic Cu−Mn−MCM-41 supported catalyst shows higher oxidation activity than either single metal catalyst, i.e., Cu−MCM-41 and Mn−MCM-41. The highly dispersed Cu−Mn mixed oxides on mesoporous structures probably provide active sites for the complete oxidation of toluene on these mesoporous catalysts.

1. Introduction

Volatile organic compounds (VOCs) emitted from industrial processes and automobile exhaust emissions are recognized as major contributions to air pollution. Catalytic combustion at a lower temperature is an effective route to eliminate VOCs.[1] A variety of catalysts have been widely investigated for the combustion of VOCs, for example, supported noble metals such as Pd/Mg−Al hydrotalcite,[2] Pd/Al_2O_3,[3] Pd/ZrO_2,[4,5] PdO/SnO_2,[6] platinum-containing monolithic carbon aerogels,[7] Pt/Al_2O_3,[8,9] supported metal oxides such as Cu−NaHY,[10] Cu/Mg/Al hydrotalcites,[11] Cu/TiO_2,[12] Zn−Co/Al_2O_3,[13] gold/cerium oxide,[14] gold/iron oxide,[15] silica-supported U_3O_8,[16] $V/MgAl_2O_4$,[17] mixed metal oxides such as Co−Fe−Cu mixed oxides,[18] Mn-doped ZrO_2,[19] and Fe-Doped ZrO_2.[20,21]

Specifically, Okumura et al. have recently reported that the oxide support might play a significant role for the Pd-supported catalysts on the catalytic combustion of toluene.[4,5] Antunes et al. have reported that CuNaHY zeolites show high toluene combustion activity and serious deactivation at low temperatures due to the formation of carbonaceous deposits (coke) retained inside the zeolite pores during the reaction process.[10] On the other hand, MCM-41 possesses high BET surface areas, uniform pore sizes with larger pore dimensions between 1.5 and 10 nm, and high thermal and hydrothermal stability.[22] Moreover, it has been recently found in our laboratory that MnOx−ZrO_2 and CuOx−MnOx mixed oxides prepared in reverse microemulsion show higher specific surface areas and superior high toluene combustion activity.[19]

Therefore, in this presentation, MCM-41-supported Cu−Mn catalysts were synthesized by direct template procedure or ion exchange of siliceous MCM-41 with Cu−Mn precursor solutions for catalytic deep oxidation of toluene. The oxidation activity results were also compared to those for conventional amorphous silica, β-zeolite, or ZSM-5-supported Cu−Mn catalysts.

2. Experimental Section

2.1 Synthesis of the Catalysts. The siliceous MCM-41 was prepared in a similar procedure as reported elsewhere[23] using the following gel composition: $(1.0SiO_2)$:(0.4CTAB):(1.6TMB):$(12.2NH_4OH)$:(53ethanol):$(171H_2O)$, where CTAB and TMB denote cetyltrimethylammonium bromide (Beijing Chemical Reagents Company) and trimethylbenzene (Fluka Company). Tetraethoxysilane (Huabei Special Chemical Reagents Center) was used as a silica precursor. These mixtures were transferred into a Teflon beaker and sealed for 24 h at 25 °C. The obtained solid material was filtered, washed, dried at 25 °C, and then calcined with a heating rate of 10 °C/min in flowing nitrogen up to 550 °C and then in air at 550 °C for 3 h. These samples are referred to as MCM-41. The thus obtained MCM-41 powders were ion exchanged with citric acid and then ion exchanged with known concentrations of aqueous solutions of $Cu(CH_3COO)_2$ (Beijing Shuanghuan Chemical Reagents Company) and $Mn(CH_3COO)_2$ (Beijing Shuanghuan Chemical Reagents Company). The final samples were denoted as CuMn/MCM-41 after being filtered, washed, dried in air at 120 °C for 24 h, and then calcined at 300−700 °C. For comparison purposes, the conventional amorphous silica, β-zeolite, and ZSM-5, supplied by Nankai University Chemical Factory, were also used as catalyst supports to prepare CuMn/SiO_2, CuMn/β-zeolite, and CuMn/ZSM-5-*x* (*x* denotes the molar ratio of SiO_2 to Al_2O_3), respectively, according to the similar ion exchange procedure above. These final samples were calcined, followed by being crushed and sieved at 100−150 meshes and then ready for the catalyst tests.

Alternatively, an appropriate amount of aqueous solutions of $Cu(CH_3COO)_2$ and $Mn(CH_3COO)_2$ were added to the gel compositions during the synthesis process of the above MCM-41 samples and therefore obtained the metal containing meso-

* Corresponding author. E-mail address: wbli@mail.tsinghua.edu.cn or wblichem@yahoo.com.cn.

† Department of Environmental Science and Engineering, Tsinghua University.

‡ Inorganic Chemistry Laboratory, University of Oxford.

10.1021/jp063580g CCC: $33.50
Published on Web 10/06/2006

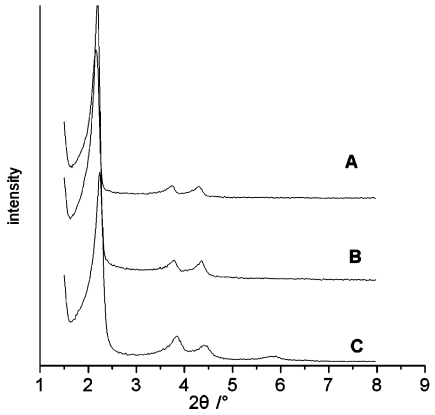

Figure 1. XRD patterns of MCM-41 (A), Cu−Mn/MCM-41−300 (B), and Cu−Mn/MCM-41-550 (C).

porous materials, i.e., Cu−MCM-41-g, Mn−MCM-41-g, and Cu−Mn−MCM-41-g.

2.2. Characterization. X-ray diffraction (XRD) patterns were obtained on Rigaku D/max RB X-ray diffractometer using Cu Kα radiation. Nitrogen adsorption and desorption isotherms were determined at −196 °C by means of Micromeritics ASAP 2010 surface area analyzer from which BET surface areas were calculated and the pore volumes were determined using the procedure proposed by Barrett, Joyner, and Halenda (BJH). Elemental analysis was performed with an X-ray fluorescence (XRF) analyzer on a Shimadzu XRF-1700 spectrometer. Thermogravimetric analysis (TGA) measurements were carried out under flowing air in a high-resolution DuPont 2100 thermogravimetric analyzer with a heating rate of 10 °C/min.

2.3. Catalytic Activities. Catalytic activities were measured in a 10 mm i.d. quartz tubular reactor. The reaction mixture consisting of toluene (0.35 vol %), O_2 (9 vol %), and argon (balance gas) was passed continuously through a 0.1 g catalyst sample bed with a total flow rate of 60 mL/min of argon. The inlet and outlet gas compositions were analyzed after stepwise changes in the reaction temperatures by an on-line gas chromatograph (Shimadzu 14B) with a FID detector using a Porapak Q column.

3. Results and Discussion

The XRD patterns illustrate that the synthesized MCM-41 sample has a typical MCM-41 mesoporous structure with three sharp peaks corresponding to Miller indices (100), (110), and (200), as shown in Figure 1. Moreover, after the sample was ion exchanged with Cu and Mn aqueous solutions and thereafter calcined at 300 °C and 550 °C, respectively, the XRD peaks remain sharp and intense for these ion-exchanged forms, i.e., Cu−Mn/MCM-41−300 and Cu−Mn/MCM-41−550, indicating that these materials have much stable and highly ordered mesoporous pore structures. In addition, it is observed that the 2θ value of the (100) diffraction peak of the ion-exchanged sample calcined at 300 °C remains unchanged, while the value of the ion-exchanged sample calcined at 550 °C slightly shifted to the high value, indicating the pore size becomes slightly smaller after calcination at a high temperature.

The mesoporous structures of the above MCM-41 and Cu−Mn/MCM-41-550 after calcinations at 550 °C were also confirmed by N_2 adsorption/desorption isotherms, as displayed in Figure 2. As typical of type IV isotherms of MCM-41 with a sharp inflection at the relative pressure (P/Po) between 0.25 and 0.40 is observed for the MCM-41 sample. In the case of the Cu−Mn/MCM-41-550 sample, it also displays an isotherm

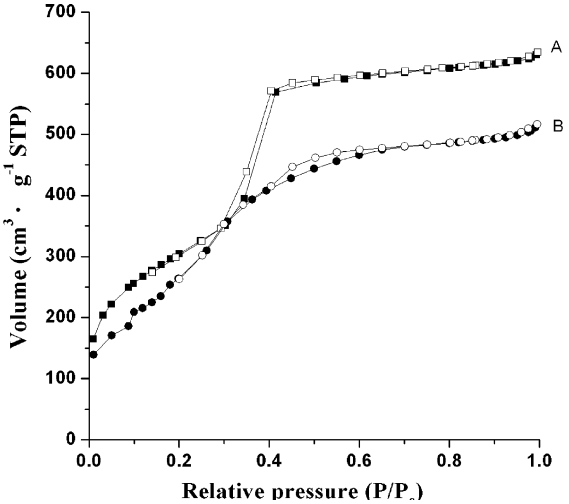

Figure 2. Nitrogen adsorption isotherms of MCM-41 (A) and Cu−Mn/MCM-41-550 (B).

TABLE 1: Chemical Compositions and Pore Structures of the Catalysts

catalyst	CuO and MnO loading (wt %) CuO	MnO	SiO_2/Al_2O_3 (molar ratio)	BET surface area (m^2/g)	pore volume (cm^3/g)
MCM41				1100	1.073
Cu−Mn/ MCM-41-550	15.60	0.72		1043	0.895
β-zeolite			100	521	0.203
CuMn/β-zeolite	16.59	1.05	100	435	0.211
amorphous silica	15.65	0.78		960	0.411

characteristic of mesoporous solids. A decrease of the height of the mesopore condensation were observed on Cu−Mn supported sample. Table 1 gives the material properties measured by N_2 adsorption/ desorption analysis and XRF analysis, which gives the Cu and Mn loading amount, SiO_2/Al_2O_3 molar ratio, BET surface areas, and pore volumes of MCM-41 and Cu−Mn/MCM-41-550, β-zeolite, and Cu−Mn/β-zeolite. The pore diameter and pore volume of the catalysts were decreased after loading Cu and Mn species (Table 1 and Figure 1). The decrease in pore volume and pore diameter could be ascribed to the Cu and Mn species supported inside the channels of the mesoporous pores. The decrease in specific surface area is also because some of the pore channels were blocked by particles of Cu and Mn species. The similar result was also reported recently on 10.5−47.5 wt % $LaCoO_3$ oxides supported on mesoporous silica by Nguyen et al.[24]

Figure 3 shows the oxidation conversion of toluene measured as a function of reaction temperatures on the various Cu−Mn catalysts with different supports, i.e., MCM-41, β zeolite, ZSM-5-25, ZSM-5-38, and porous silica. Elemental analysis of all of these samples shows that the loading amount of CuO and MnO was around 16 and 1 wt %, respectively. It is clear that Cu−Mn/MCM-41 shows the lowest light-off temperature and highest oxidation activity, e. g., 90% of toluene conversion into CO_2 at 320 °C. It is also shown that the sequences of oxidation conversion activities at high temperatures follow the order Cu−Mn/MCM-41 > Cu−Mn/ZSM-5-25 > Cu−Mn/ZSM-5-38 > Cu−Mn/β-zeolite > Cu−Mn/porous silica. For example, the oxidation conversions at 400 °C are 99.6%, 92.1%, 85.6%, 68.2%, and 36.4% on Cu−Mn/MCM-41, Cu−Mn/ZSM-5-25, Cu−Mn/ZSM-5-38, Cu−Mn/β zeolite, and Cu−Mn/porous silica, respectively. The highest oxidation activity of Cu−Mn/MCM-41 is probably related with the unique pore structure and the uniform dispersion of Cu and Mn species on the catalysts.

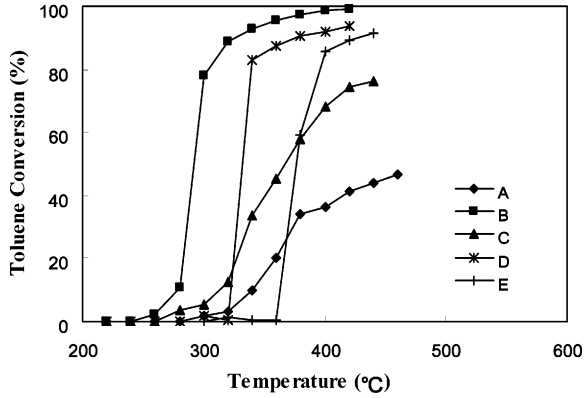

Figure 3. Oxidation conversion of toluene as a function of reaction temperature on Cu−Mn/porous SiO_2 (A), Cu−Mn/MCM-41 (B), Cu−Mn/β-zeolite (C), Cu−Mn/ZSM-5-25 (D), and Cu−Mn/ZSM-5-38 (E).

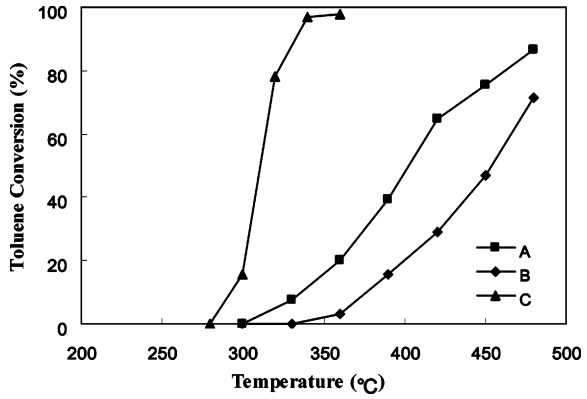

Figure 4. Oxidation conversion of toluene as a function of reaction temperatures on Cu−MCM-41-g (A), Mn−MCM-41-g (B), and Cu−Mn−MCM-41-g (C).

More recently, Williams et al. have reported that lower ignition temperatures were observed for oxidation of toluene in waste gas streams on mesoporous Ti−HMS catalysts with increasingly higher textural porosities, which indicates that textural porosity has a significant positive effect on catalyst performance.[25]

To gain an insight on the active species of either Cu or Mn, the single metal aqueous solution or their mixed solution was directly added to gel compositions when preparing mesoporous materials and hence obtain the Cu−MCM-41-g, Mn−MCM-41-g, and CuMn−MCM-41-g catalysts. These materials prepared show a good degree of crystallinity with a regular ordering of the mesoporous pore structures, which are similar to that in Figure 1C. Chemical analysis shows that 15.8% Cu and 15.2% Mn were supported on Cu−MCM-41-g and Mn−MCM-41-g, respectively, and 14.5% Cu and 0.85% Mn were supported on CuMn−MCM-41-g. Figure 4 shows the catalytic activities of toluene oxidation measured as a function of reaction temperature on the Cu−MCM-41-g, Mn−MCM-41-g, and Cu−Mn−MCM-41-g catalysts after calcination at 550 °C. It demonstrates that catalytic conversion of toluene on CuMn−MCM-41-g is much higher than that on either Cu−MCM-41-g or Mn−MCM-41-g. For example, 99% of the conversion of toluene was obtained at 340 °C on CuMn−MCM-41-g as compared to 86% of the conversion at 480 °C on Cu−MCM-41-g and 72% at 480 °C on Mn−MCM-41-g.

Figure 5 presents the XRD patterns of the Cu−Mn/MCM-41 samples calcined at 300, 550, and 800 °C. It is clear that mesoporous structures remains unchanged after the samples were calcined at 550 and 800 °C (Figure 5A); while the 2θ value of the (100) diffraction peak of the sample calcined at

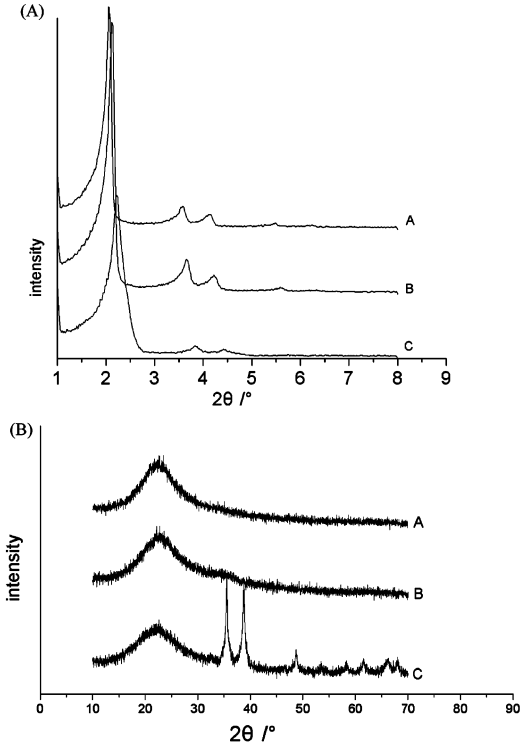

Figure 5. XRD patterns of the Cu−Mn/MCM-41 calcined at 300 °C (A), 550 °C (B), and 800 °C (C).

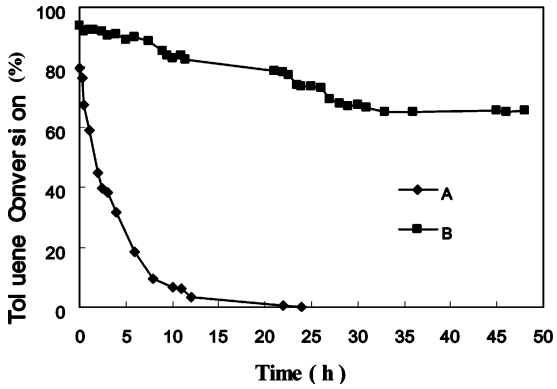

Figure 6. Toluene conversion as a function of time-on-stream on Cu−Mn/β-zeolite at 400 °C (A) and Cu−Mn/MCM-41 at 320 °C (B).

550 °C was almost the same as the value on the sample calcined at 300 °C, indicating the pore structure remained the same. Further heating to 800 °C led to the 2θ value moving to a high value, indicating that the pore size became smaller. On the other hand, only a minor amount of Cu and Mn species were observed on the sample calcined above 550 °C; heating the sample to 800 °C shows the predominant amount of CuO and spinel $CuMn_2O_4$ exists on the sample (Figure 5B), considering that the $CuMn_2O_4$ nanostructured catalysts are more active than either single copper oxide or manganese oxide, as found in our lab. It was suggested that the highly dispersed structures of CuO and $CuMn_2O_4$ were supported on MCM-41, as evidenced by XRD, are possibly responsible for the high acivity of the oxidation reaction.

Toluene conversion versus time-on-stream on Cu−Mn/MCM-41 and Cu−Mn/β-zeolite catalysts is illustrated in Figure 6. It is found that toluene conversion on Cu−Mn/MCM-41 at 320 °C was initially 94%, then slowly reached 82% after running for 24 h, and finally stabilized at 64% after running 28−48 h. On the other hand, the toluene conversion on Cu−Mn/β-zeolite at 400 °C was initially 80%, then quickly decreased to 42%

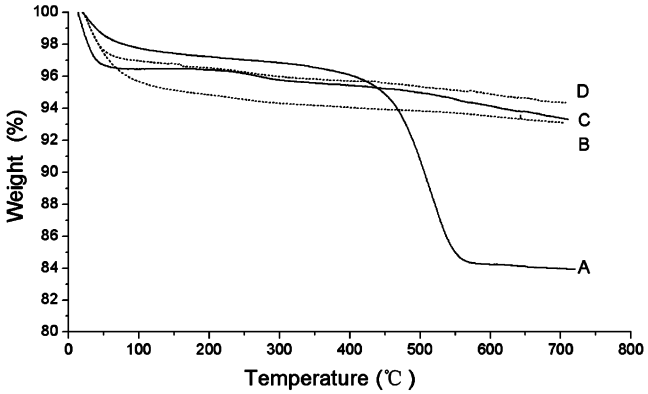

Figure 7. TGA profiles of Cu−Mn/β-zeolite-used (A), Cu−Mn/βzeolite (B), Cu−Mn/MCM-41-used (C), and Cu−Mn/MCM-41 (D).

within 1 h and then completely deactivated after running for 12−24 h. The similar deactivation results were also observed on Pt/β-zeolite catalysts between 200 and 220 °C by Tsou.[26] Meanwhile, it is noted that the color of Cu−Mn/MCM-41 did not change while the Cu−Mn/β-zeolite sample turn to black. Apparently, the coke deposition on the Cu−Mn/β-zeolite sample is closely related with the deactivation of the catalyst.[10,26] The used catalyst after the reaction was denoted as Cu−Mn/β-used and Cu−Mn/MCM41-used, respectively.

Thermogravimetric analysis (TGA) was employed for the calcination of Cu−Mn/β-used, Cu−Mn/MCM41-used as well as the fresh Cu−Mn/β-zeolite, Cu−Mn/MCM-41 in an air flow (Figure 7). For the Cu−Mn/MCM41-used sample, the total amount of weight loss at 700 °C is ca. 6.67 wt %, which exhibits little difference with the value of 5.66 wt % on the fresh Cu−Mn/MCM41 sample, indicating no coking exits on the sample. However, for Cu−Mn/β-used, two distinct stages of weight loss are observed: Below 100 °C, about 1.7 wt % of water is desorbed from Cu−Mn/β-used, while the fresh Cu−Mn/β releases about 4.4 wt % of water during this stage. Between 400 and 550 °C, the second weight loss on Cu−Mn/β-used is ascribed to the coke decomposition and combustion in air flow as compared to no distinct weight loss detected on the fresh Cu−Mn/β-zeolite. Considering the differences of oxidation activities between Cu−Mn/β and Cu−Mn/MCM-41, it is reasonable to conclude that coke formation plays a key role in the deactivation of the catalyst, and coke formation could be successfully minimized on the Cu−Mn/MCM-41 sample and hence keep the high reaction activity of oxidation of toluene as compared to abrupt loss of the activity on Cu−Mn/β-zeolite.

4. Conclusion

In this presentation, Cu−Mn containing mesoporous and microporous catalysts were used for the complete oxidation of toluene. First, the mesoporous catalysts showed the highest catalytic activity as compared to microporous catalysts and supported porous silica. Probably the lower amount of coke formation due to the unique mesoporous structures will possibly play a key role in the high activity on the mesoporous catalyst. Second, Cu−Mn−MCM-41 shows higher activity than either single metal catalyst, i.e., Cu−MCM-41 and Mn−MCM-41. The highly dispersed Cu−Mn mixed oxides on mesoporous structure possibly provide active sites for the complete oxidation of toluene on the mesoporous catalysts. It seems that these supported mesoporous catalysts are very useful to develop a type of catalysts for complete oxidation of aromatic compounds to avoid the severe problems associated with the coke formation during the reaction process. Further work to optimize the loading amount of copper and manganese on the catalysts is in progress in our lab in order to increase reaction activities for the deep oxidation of toluene.

Acknowledgment. W.B.L. thanks the Royal Society from the UK for a research fellowship and the Natural Science Foundation of China (no. 20277023) for partial financial support.

References and Notes

(1) Spivey, J. J. *Ind. Eng. Chem. Res.* **1987**, *26*, 2165.
(2) Carpentier, J.; Lemonier, J. F.; Siffert, S.; Laversin, H.; Aboukais, A. *Appl. Catal., A* **2002**, *234*, 91.
(3) Paulis, M.; Gandia, L. M.; Gil, A.; Sambeth, J.; Odriozola, J. A.; Montes, M. *Appl. Catal, B* **2000**, *26*, 37.
(4) Okumura, K.; Kobayashi, T.; Tanaka, H.; Niwa, M. *Appl. Catal., B* **2003**, *44*, 325.
(5) Okumura, K.; Tanaka, H.; Niwa, M. *Catal. Lett.* **1999**, *58*, 43.
(6) Takeguchi, T.; Aoyama, S.; Ueda, J.; Kikuchi, R.; Eguchi, K. *Top. Catal.* **2003**, *23*, 159.
(7) Maldonado-Hodar, F. J.; Moreno-Castilla, C.; Perez-Cadenas, A. F. *Appl. Catal., B* **2004**, *54*, 217.
(8) Ordóñez, S.; Bello, L.; Sastre, H.; Rosal, R.; Diez, F. V. *Appl. Catal., B* **2002**, *38*, 139.
(9) Paulis, M.; Peyrard, H.; Montes, M. *J. Catal.* **2001**, *199*, 30.
(10) Antunes, A. P.; Ribeiro, M. F.; Silva, J. M.; Ribeiro, F. R.; Magnoux, P.; Guisnet, M. *Appl. Catal., B* **2001**, *33*, 149.
(11) Kovanda, F.; Jiratova, K.; Rymes, J.; Kolousek, D. *Appl. Clay Sci.* **2001**, *18*, 71.
(12) Larsson, P.-O.; Andersson, A. L.; Wallenberg, R.; Svensson, B. *J. Catal.* **1996**, *163*, 279.
(13) Klissurski, D.; Uzunova, E.; Yankova, K. *Appl. Catal., A* **1993**, *95*, 103.
(14) Scirè, S.; Minicò, S.; Crisafulli, C.; Satriano, C.; Pistone, A. *Appl. Catal., B* **2003**, *40*, 43.
(15) Minicò, S.; Scirè, S.; Crisafulli, C.; Galvagno, S. *Appl. Catal., B* **2001**, *34*, 277.
(16) Taylor, S. H.; Heneghan, C. S.; Hutchings, G. J.; Hudson, I. D. *Catal. Today* **2000**, *59*, 249.
(17) Evans, O. R.; Bell, A. T.; Tilley, T. D. *J. Catal.* **2004**, *226*, 292.
(18) Carpentier, J.; Lamonier, J. F.; Siffert, S.; Laversin, H.; Aboukais, A. *Stud. Surf. Sci. Catal.* **2002**, *142*, 1197.
(19) Li, W. B.; Chu, W. B.; Zhuang, M.; Hua, J. *Catal. Today* **2004**, 93, 205.
(20) Choudhary, V. R.; Deshmukh, G. M.; Mishra, D. P. *Energy Fuels* **2005**, *19*, 54.
(21) Choudhary, V. R.; Deshmukh, G. M.; Pataskar, S. G. *Catal. Commun.* **2004**, *5*, 115.
(22) Kresge, C. T.; Leonowicz, M. E.; Roth, W. J.; Vartuli, J. C.; Beck, J. S. *Nature* **1992**, *359*, 710.
(23) Li, W. B.; Zhang, Y.; Lin, Y.; Yang, X. *Stud. Surf. Sci. Catal.* **2002**, *141*, 503.
(24) Nguyen, S. V.; Szabo, V.; Trong On, D.; Kaliaguine, S. *Microporous Mesoporous Mater.* **2002**, *54*, 51.
(25) Williams, T.; Beltramini, J.; Lu, G. Q. *J. Environ. Eng. (Reston, VA, U.S.)* **2004**, *130* (3), 356.
(26) Tsou, J.; Pinard, L.; Magnoux, P.; Figueiredo, J. L.; Guisnet, M. *Appl. Catal., B* **2003**, *46*, 371.